

Nanomagnetic Competition Assay for Low-Abundance Protein Biomarker Quantification in Unprocessed Human Sera

Yuanpeng Li,[†] Balasubramanian Srinivasan,[‡] Ying Jing,[†] Xiaofeng Yao,^{†,§} Marie A. Hugger,[‡] Jian-Ping Wang,^{*,†} and Chengguo Xing^{*,‡}

Department of Electrical and Computer Engineering, and Department of Medicinal Chemistry, University of Minnesota, Minneapolis, Minnesota 55455

Received December 17, 2009; E-mail: jpwang@umn.edu; xingx009@umn.edu

Abstract: A novel giant magnetoresistive sensor and uniform high-magnetic-moment FeCo nanoparticles (12.8 nm)-based detecting platform with minimized detecting distance was developed for rapid biomolecule quantification from body fluids. Such a system demonstrates specific, accurate, and quick detection and quantification of interleukin-6, a low-abundance protein and a potential cancer biomarker, directly in 4 μ L of unprocessed human sera. This platform is expected to facilitate the identification and validation of disease biomarkers. It may eventually lead to a low-cost personal medical device for chronic disease early detection, diagnosis, and prognosis.

Introduction

Traditional technologies for disease biomarker detection are enzyme-linked immunosorbent assays (ELISA),¹ Western blotting, immunohistochemistry, DNA-based genomics, and mass spectrometry-based proteomics and metabolomics.² With no exception, these approaches have intrinsic common limitations, including expensive equipment, long processing time, extensive professional training, and low signal-to-noise ratio.³ Methods that can rapidly and specifically quantify disease biomarkers from unprocessed human body fluids with low cost is expected to greatly facilitate disease biomarker validation and disease early detection. Sensing based on the combination of giant magnetoresistive (GMR) sensors and magnetic nanoparticles has attracted much attention as a promising alternative,^{4–14} since such a system has the unique merits of portability,⁷ low cost,⁸ rapid detection,⁹ ease for integration into lab-on-a-chip systems,¹⁰ and lack of magnetic background in biological samples. Nevertheless, most GMR biosensor application has been confined to proof of detecting concept,¹¹ model studies,¹² or detection of spiked biomolecules, or only in animal samples, the integrated testing conditions have not been confirmed for the physiologically relevant ones, e.g. for unprocessed human samples,^{7,13,14} mainly because its theoretical sensitivity, specificity and monotonicity have not been achieved under physiological conditions for unprocessed human samples.

This study reports the first realization of specific, accurate, and rapid quantification of interleukin-6 (IL-6), a low-abundance protein and a potential cancer biomarker,¹⁵ in unprocessed human sera, by employing our novel GMR sensor with our

uniform high-magnetic-moment FeCo nanoparticles and minimizing the detecting distance between nanoparticles and GMR sensing. Such integration led to significant improvement in detecting sensitivity and accuracy. The near 0° magnetization design of the GMR sensor also eliminates the need for a high magnetic field for detection, which opens the opportunity for portable device. Our platform therefore has a significant impact on magnetic sensor-based biomolecule detection with the potential to develop a lab-on-a-chip device, practical for frequent biomarker detection and monitoring.

Results and Discussion

Sensitivity and Accuracy Enhancement with a Novel GMR Sensor and Usage of Uniform High-Magnetic-Moment FeCo Nanoparticles. With respect to the GMR transfer curve, most groups seek high linearity by employing a 90° ground state for the device magnetization direction.^{5–13} This configuration, however, generally has 3 times lower sensitivity compared to a

- (4) (a) Baibich, M. N.; Broto, J. M.; Fert, A.; Nguyen Van Dau, F.; Petroff, F.; Etienne, P.; Creuzet, G.; Friederich, A.; Chazelas, J. *Phys. Rev. Lett.* **1988**, *61*, 2472–2475. (b) Binasch, G.; Grünberg, P.; Saurenbach, F.; Zinn, W. *Phys. Rev. B* **1989**, *39*, 4828–4830.
- (5) Baselt, D. R.; Lee, G. U.; Natesan, M.; Metzger, S. W.; Sheehan, P. E.; Colton, R. J. *Biosens. Bioelectron.* **1998**, *13*, 731–739.
- (6) Tamanaha, C. R.; Mulvaney, S. P.; Rife, J. C.; Whitman, L. J. *Biosens. Bioelectron.* **2008**, *24*, 1–13.
- (7) (a) Osterfeld, S. J.; Yu, H.; Gaster, R. S.; Caramuta, S.; Xu, L.; Han, S.-J.; Hall, D. A.; Wilson, R. J.; Sun, S.; White, R. L.; Davis, R. W.; Pourmand, N.; Wang, S. X. *Proc. Natl. Acad. Sci. U.S.A.* **2008**, *105*, 20637–20640. (b) Gaster, R. S.; Hall, D. A.; Nielsen, C. H.; Osterfeld, S. J.; Yu, H.; Mach, K. E.; Wilson, R. J.; Murmann, B.; Liao, J. C.; Gambhir, S. S.; Wang, S. X. *Nature Medicine* **2009**, *15*, 1327–1332. (c) Martins, V. C.; Germano, J.; Cardoso, F. A.; Loureiro, J.; Cardoso, S.; Sousa, L.; Piedade, M.; Fonseca, L. P.; Freitas, P. P. *J. Magn. Mater.* **2009**, in press (available at <http://dx.doi.org/10.1016/j.jmmm.2009.02.141>).
- (8) De Boer, B. M.; Kahlman, J. A. H. M.; Jansen, T. P. G. H.; Duric, H.; Veen, J. *Biosens. Bioelectron.* **2007**, *22*, 2366–2370.
- (9) Sandhu, A. *Nat. Nanotechnol.* **2007**, *2*, 746–748.
- (10) Rife, J. C.; Miller, M. M.; Sheehan, P. E.; Tamanaha, C. R.; Tondra, M.; Whitman, L. J. *Sens. Actuators A* **2003**, *107*, 209–218.

[†] Department of Electrical and Computer Engineering.

[‡] Department of Medicinal Chemistry.

[§] Current address: Western Digital, Lake Forest, CA.

- (1) (a) Mitchell, P. *Nat. Biotechnol.* **2002**, *20*, 225–229. (b) Chan, S. M.; Ermann, J.; Su, L.; Fathman, C. G.; Utz, P. *J. Nat. Med.* **2004**, *10*, 1390–1396.
- (2) Diamandis, E. P. *Mol. Cell. Proteins* **2004**, *3*, 367–378.
- (3) Engvall, E.; Perlmann, P. *Immunochemistry* **1971**, *8*, 871–874.

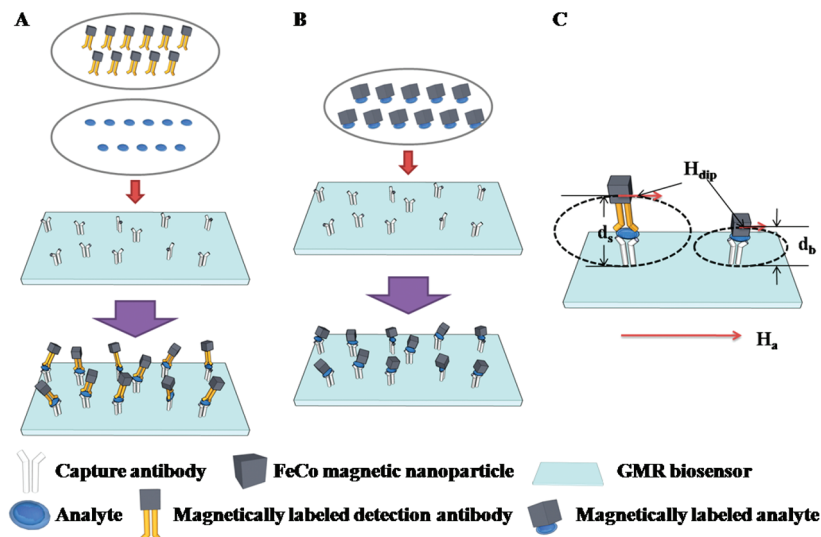


Figure 1. Two GMR sensor and magnetic nanoparticle-based biomolecule detection schemes. (A) Three-layer (sandwich) approach: the GMR sensors are first functionalized with capture antibodies. The analyte binds to the capture antibody. Subsequently, detection antibodies labeled with magnetic nanoparticles are then applied and bind to the captured analyte. (B) Two-layer approach: after the functionalization of the GMR sensor with capture antibodies, the magnetic nanoparticle-modified analyte is directly applied and captured on the GMR biosensors. (C) GMR biosensor working principle. The GMR biosensor can detect the dipole field generated by the magnetic nanoparticles captured on the sensor surface, which is sensitive to distance (Supporting Information, p S4).

GMR sensor with a near 0° ground state.¹⁴ Moreover, a GMR sensor with a near 0° ground state would require a much lower working field (10 Oe) compared to the GMR sensor with a 90° ground state (80 Oe or more), more amenable for low cost and portability.¹⁴ The GMR sensors used in this study therefore have a near 0° ground state for magnetization.

With respect to nanoparticles, high magnetic moment leads to increased signal, thereby higher sensitivity. We have pioneered the design, implementation, and application of high-magnetic-moment nanoparticles for biosensing.^{14,16,17} With the same nanoparticle volume, the net magnetic moment of one FeCo nanoparticle is 7–11 times higher than that of one Fe₃O₄ nanoparticle (commercialized) at an applied field of 10 Oe (Supporting Information, Table S1). Regarding nanoparticle uniformity, the magnetic signal depends on the size and shape of the particle. Thus, homogeneity of magnetic nanoparticles is critical for accurate quantification, especially for low-abundance proteins, because signal heterogeneity introduced by non-homogenous nanoparticles can lead to significant quantification error. Our high-magnetic-moment FeCo nanoparticles are highly homogeneous in size (12.8 ± 1.58 nm) and shape (cubic).¹⁴ We thus expect that quantification of low-abundance proteins would be more accurate with our uniform high-magnetic-moment FeCo nanoparticles.

Sensitivity and Monotonicity of Two-Layer Detection and Three-Layer Detection.

Based on the detecting principle,⁵ the sensitivity of a GMR sensor strongly depends on the distance (d) between the center of the magnetic particle and the free layer of the sensor: the magnetic signal decreases as the distance increases, the signal being proportional to $1/d^3$ (Supporting Information, p S4). Currently, all GMR detection of protein-based biomolecules employs a three-layer (sandwich)-based approach (Figure 1A).^{5–14} This increases the distance between the nanoparticle and sensor by incorporating a detecting antibody, compared to a two-layer approach (Figure 1B,C), thus compromising the detection sensitivity (a two-layer approach theoretically would enhance the detecting sensitivity over the three-layered approach by 3.4–39 times, depending on the size and orientation of the antibodies and biomolecule; for details, see Supporting Information, p S4). Moreover, the signal detected by the three-layer approach does not necessarily provide a 1:1 correspondence between signal and biomarker concentration as the two-layer competition approach would do (Supporting Information, Figures S1 and S2), limiting its usage to unequivocally quantify proteins from unprocessed body fluid, given the high abundance variation of any proteins in body fluid among different individuals.¹⁵

As shown in Figure 2, our device can detect IL-6 at a concentration as low as 20.76 pM using the three-layer approach (the densities of both capture antibodies and detection antibodies have been optimized to maximize its sensitivity, see Supporting Information, pp S7–S9). In contrast, the detecting sensitivity of our device based on the two-layer approach reaches 373 fM for IL-6, 55 times more sensitive than the three-layer approach. These results confirmed the superior detecting sensitivity of the two-layer approach over the traditional three-layer approach.

- (11) (a) Janssen, X. J. A.; Van Ijzendoorn, L. J.; Prins, M. W. J. *Biosens. Bioelectron.* **2008**, *23*, 833–838. (b) Wirix-Speetjens, R.; Fyen, W.; Boeck, J.; Borghs, G. *J. Appl. Phys.* **2006**, *99*, 103903. (c) Schotter, J.; Kamp, P. B.; Becker, A.; Pühler, A.; Reiss, G.; Brückl, H. *Biosens. Bioelectron.* **2004**, *19*, 1149–1156. (d) Graham, D. L.; Ferreira, H.; Bernardo, J.; Freitas, P. P.; Cabral, J. M. S. *J. Appl. Phys.* **2002**, *91*, 7786–7788.
- (12) (a) Li, G.; Wang, S. X. *IEEE Trans. Magn.* **2003**, *39*, 3313–3315. (b) Nordling, J.; Millen, R. L.; Bullen, H. A.; Porter, M. D.; Tondra, M.; Granger, M. C. *Anal. Chem.* **2008**, *80*, 7930–7939.
- (13) Mulvaney, S. P.; Myers, K. M.; Sheehan, P. E.; Whitman, L. J. *Biosens. Bioelectron.* **2009**, *24*, 1109–1115.
- (14) Srinivasan, B.; Li, Y.; Jing, Y.; Xu, Y.; Yao, X.; Xing, C.; Wang, J.-P. *Angew. Chem., Int. Ed.* **2009**, *48*, 2764–2767.

- (15) Anderson, N. L.; Anderson, N. G. *Mol. Cell. Proteomics* **2002**, *1*, 845–867.

- (16) Bai, J.; Xu, Y.; Wang, J.-P. *IEEE Trans. Magn.* **2007**, *43*, 3340–3342. (17) Xu, Y.; Bai, J.; Wang, J.-P. *J. Magn. Magn. Mater.* **2007**, *311*, 131–134.

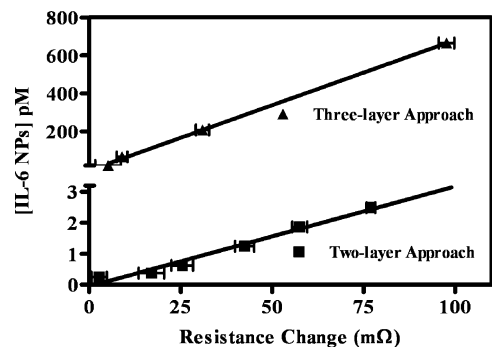


Figure 2. Sensitivity differences between sandwich and two-layer detecting approaches by comparing their dose–response curves. Data points, mean; bar, standard deviation ($6 \leq n \leq 10$). For the sandwich approach, the same amount of detection antibody-modified FeCo magnetic nanoparticles was applied to each sensor with different amounts of unlabeled IL-6 molecules. For the two-layer approach, different amounts of FeCo magnetic nanoparticle labeled with IL-6 molecules were applied on each sensor.

Competition-Based IL-6 Quantification in Unprocessed Human Sera. To practically employ the two-layer approach for IL-6 quantification in unknown samples, we developed a two-layer competition-based approach (Figure 3A) and established the dose–response curve. Briefly, a mixture of 4.15 pM magnetic nanoparticle-labeled (MNL) IL-6 molecules and varied concentrations of unlabeled IL-6 (4 μ L) was applied onto the GMR sensor surface with signal measured. Figure 3B shows the dose–response curve of the competition detection approach, which provides a wide detection range of IL-6 from 125 fM to 41.5 pM. We also demonstrated that the testing background (either buffer or serum) has no effect on IL-6 detection and quantification (Supporting Information, Figure S8) and that the dose–response curve established under buffer background can be utilized for the quantification of IL-6 in sera.

The concentrations of IL-6 in human serum samples were then quantified following this two-layer competition-based approach. Ten human serum samples were evaluated. Five of them were from healthy individuals, which were labeled NS1–NS5. The other five were from lung cancer patients, labeled CS1–CS5 (Supporting Information, Table S3). Briefly, MNL IL-6 molecules (4.15 pM) were mixed with the unprocessed human serum sample (4 μ L) and applied onto the GMR sensor surface (\sim 4 nL of unprocessed human serum per sensor area). The concentration of IL-6

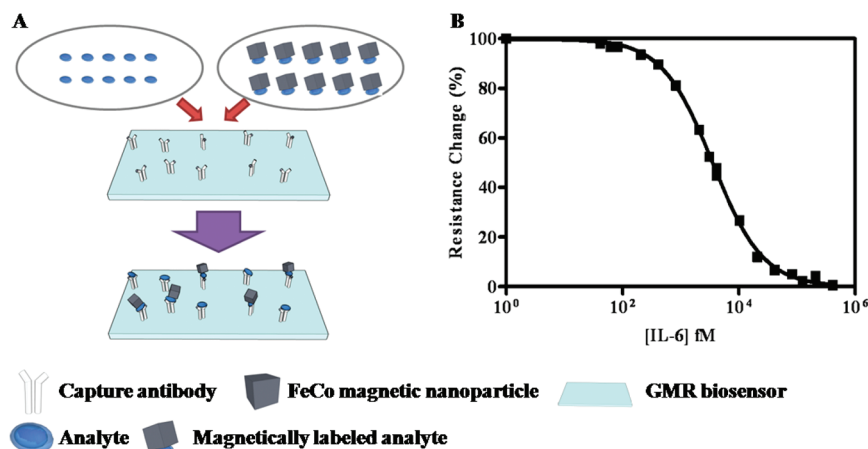


Figure 3. (A) Competition-based two-layer detection scheme: the magnetic MNL IL-6 and unlabeled IL-6 are applied on the capture antibody-functionalized GMR biosensor and compete for the binding sites. (B) Two-layer competition-based dose–response curve between 4.15 pM FeCo MNL IL-6 and varied concentrations of unlabeled IL-6 molecules. The solid curve is the nonlinear dose fitting curve. Data points, mean; bars, standard deviation ($5 \leq n \leq 8$). Resistance change is statistically significant for IL-6, ranging from 125 fM to 41.5 pM in comparison to control sensors and background.

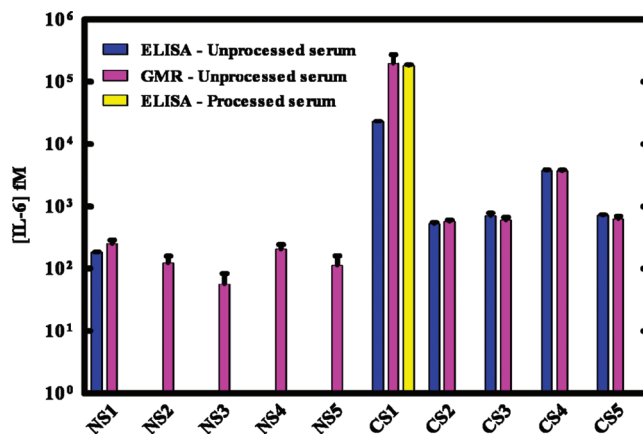


Figure 4. Comparison of IL-6 levels in human serum samples determined by ELISA and competition-based GMR biosensor. Columns, mean; bars, standard deviation ($2 \leq n \leq 8$); NS1–NS5 represent human serum samples from five healthy individuals; CS1–CS5 represent human serum samples from five lung cancer patients (see Supporting Information, p S12 for detailed information about the serum samples). “Processed serum” means that CS1 was diluted 80 times for ELISA quantification, while “unprocessed serum” means the serum sample was evaluated as such. ELISA failed to detect IL-6 in NS2–NS5.

Table 1. Comparison of IL-6 Levels in Human Serum Samples Determined by ELISA and GMR Biosensor

	[IL-6], fM									
	NS1	NS2	NS3	NS4	NS5	CS1	CS2	CS3	CS4	CS5
ELISA	219	N/A ^a	N/A ^a	N/A ^a	N/A ^a	192 140 ^b	552 742	3928 757		
GMR	248	122	56	203	112	195 981	567 597	3681 627		

^a Not detectable by ELISA. ^b After 80-fold dilution.

in sera was determined by using the above established competition-based dose–response curve (Figure 3B). Figure 4 compares the levels of IL-6 in human sera quantified by our GMR system and by commercial ELISA (R&D systems). A significant amount of IL-6 can be detected and quantified by our GMR system in all 10 unprocessed serum samples, while ELISA failed to detect IL-6 in four of the five sera from healthy individuals, NS2–NS5. The levels of IL-6 in sera NS1 and CS2–CS5 quantified by our GMR sensor are comparable to those determined by ELISA. However, there is a significant discrepancy of IL-6 abundance in unprocessed

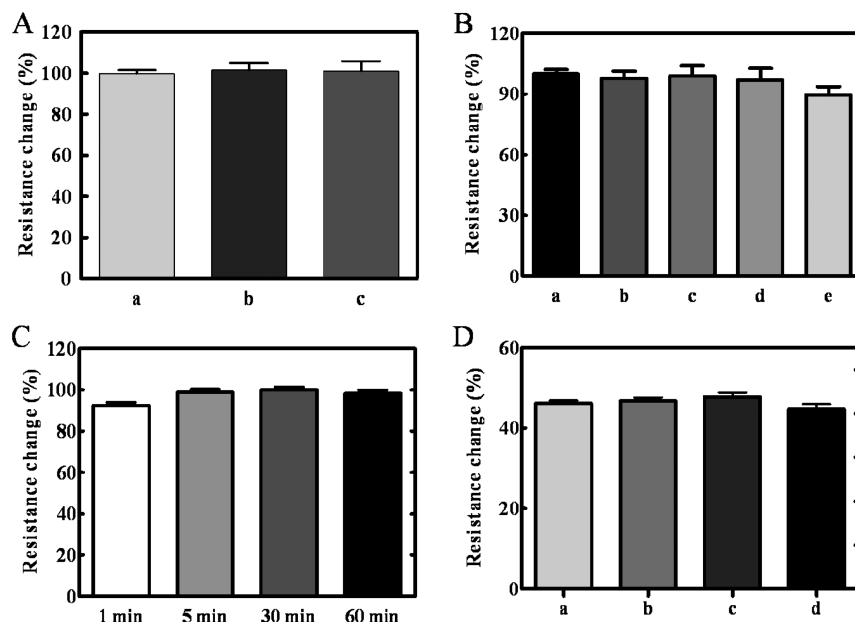


Figure 5. Detecting specificity, dynamics, and reproducibility. (A) Resistance change in the absence or presence of IL-6-depleted serum with MNL IL-6 molecules: (a) control, no IL-6-depleted serum; (b) IL-6-depleted serum from NS1; (c) IL-6-depleted serum from CS1. Columns, mean; bars, standard deviation; $n \geq 2$. Comparison among groups a–c showed no statistically significant difference. (B) Resistance change in the presence of other proteins with MNL IL-6 molecules (1.25 pM MNL IL-6): (a) control, no competition; (b) $1.25 \times 10^6 \text{ pM}$ IL-8; (c) $1.25 \times 10^6 \text{ pM}$ VEGF; (d) $1.25 \times 10^6 \text{ pM}$ FAS; (e) $1.25 \times 10^{10} \text{ pM}$ HAS. Columns, mean; bars, standard deviation ($n \geq 4$). Comparison among groups a–e showed no statistically significant difference. (C) Time course binding study. Columns, mean; bars, standard deviation; $n = 4\text{--}5$. (D) Resistance change due to competition of unlabeled recombinant human IL-6 with MNL IL-6 molecules on the sensor surface: (a–d) competition results from four independent experiments that were performed with a 1-week interval between two experiments. Columns, mean; bars, standard deviation; $n = 5\text{--}8$. Comparison among groups a–d showed no statistically significant difference.

serum CS1 between the results from ELISA ($2.42 \times 10^4 \text{ fM}$) and our device ($1.96 \times 10^5 \text{ fM}$). We hypothesize that the IL-6 level in CS1 is relatively high, out of the linear detecting range of ELISA, and that the result from ELISA underestimates the quantity of IL-6 in CS1. To test this hypothesis, serum CS1 was diluted 80 times based on our GMR data so that the level of IL-6 would be within ELISA's linear detecting range. The diluted sample was then re-evaluated by ELISA. The ELISA result from this diluted measurement ($1.92 \times 10^5 \text{ fM}$) agreed nicely with our GMR data (Figure 4, Table 1), demonstrating the accuracy and wide detecting range of our GMR sensor-based detecting system. Excitingly, the levels of IL-6 in the five sera from lung cancer patients are all significantly higher than those in the sera from healthy individuals, preliminarily supporting IL-6 as a potential lung cancer biomarker.

Detection Specificity. We then performed a series of experiments to examine the detecting specificity of our device. One approach for evaluating the detecting specificity to IL-6 in sera was to determine whether serum samples depleted of IL-6 would introduce any signals. IL-6 in serum samples NS1 and CS1 was depleted by an immunoprecipitation approach (Supporting Information, p S12). The depleted sera were then used in competition with MNL IL-6, following the same procedure. The results (Figure 5A) demonstrate that IL-6-depleted sera, irrespective of their disease state and original IL-6 level, show no competition at all against MNL IL-6, establishing the detecting specificity of our device to IL-6. The detecting specificity against other specific serum proteins of varied abundance was also evaluated. MNL IL-6 was mixed with 10^6 -fold human recombinant interleukin-8 (IL-8), human vascular endothelial growth factor (VEGF), human recombinant fatty acid synthase (FAS), or 10^{10} -fold human serum albumin (HAS) for competition detection. Again, we detected no signal changes

due to the nonspecific binding of these serum proteins, even when they are in high excess compared to IL-6 (Figure 5B).

Detection Time and Reproducibility. Finally, the detection time and reproducibility of our biosensing system were preliminarily evaluated. The time course for binding of MNL IL-6 to the GMR sensor was studied. As shown in Figure 5C, 94% signal was achieved within 1 min, and the binding reached equilibrium for quantification within 5 min, demonstrating the feasibility to realize quick detection. The system also demonstrates high reproducibility, as shown in Figure 5D: different GMR sensors, when used to quantify 4.15 pM IL-6 at four different time points, produce the same results.

Experimental Methods

GMR Sensor and High-Magnetic-Moment Nanoparticle Fabrication and Magneto-resistance Measurement. Fabrication of GMR sensor and nanoparticles and magneto-resistance measurements were carried out following the same procedures as described in our earlier report.¹⁴

Sensor Surface Modification. The GMR sensor surface was sequentially modified with (3-aminopropyl)triethoxysilane (APTES) followed by capture antibody attachment through 1-[3-(dimethylamino)propyl]-3-ethylcarbodiimide (EDC) coupling chemistry. After each step, the surface was thoroughly washed with water to remove unbound ligands, which were collected for quantification. For each step of modification, bound ligands were quantified using the following equation: amount of bound ligand on the surface = amount of total ligand added – amount of ligand recovered (for detailed procedures, see Supporting Information).

Cubic FeCo Nanoparticle Surface Modification. i. APTES Modification. A solution of APTES ($100 \mu\text{g}$ in $500 \mu\text{L}$ of ethanol) and ammonium hydroxide ($5 \mu\text{L}$, 29%) was added to cubic FeCo nanoparticles ($100 \mu\text{g}$) and sonicated for 4 h.

ii. Human Recombinant IL-6 Modification. To a dispersion of APTES-modified nanoparticles ($300 \mu\text{L}$, PBS buffer, pH 7.2;

30 μg of FeCo) were added dylight 488-labeled human recombinant IL-6 (10 μL , 100 $\mu\text{g}/\text{mL}$ in PBS buffer, pH 7.4) and EDC (10 μL , 5 mg/mL in PBS, pH 7.4), and the mixture was shaken overnight at 4 $^{\circ}\text{C}$ under light-protected conditions.

iii. IL-6 Detection Antibody Modification. To a dispersion of APTES-modified nanoparticles (250 μL , PBS buffer, pH 7.2; 25 μg of FeCo) were added dylight 488-labeled antihuman IL-6 antibody (7 μL , 1 mg/mL in PBS buffer, pH 7.4) and EDC (100 μL , 10 mg/mL in PBS, pH 7.4), and the mixture was shaken overnight at 4 $^{\circ}\text{C}$ under light-protected conditions.

After each modification, nanoparticles were harvested by an external magnet, and modified nanoparticles were thoroughly washed with water to remove unbound ligands for quantification (see Supporting Information, p S9).

Three-Layer Assay for Human IL-6 Detection. Varied concentrations of IL-6 were added to capture antibody-modified sensors (20.8 pM –2.08 nM). After that, the optimal MNL detection antibody for IL-6 was applied. Control sensors without capture antibody were used to determine any nonspecific binding of detection antibody–nanoparticle conjugate (see Supporting Information, p S10).

Two-Layer Assay for Human IL-6 Detection. Varied concentrations of MNL IL-6 were added to capture antibody-modified sensor spots (250–2500 fM). Control sensors without capture antibody were used to determine any nonspecific binding (see Supporting Information, p S10).

Competition-Based Two-Layer Assay for Human IL-6. MNL IL-6 (1.67×10^{-20} mol per sensor area, 41.5 pM) was mixed with 4 μL of human serum (4 nL per sensor area) to compete for 1.67×10^{-20} mol of capture antibodies (per sensor area) on the sensor surface (see Supporting Information, p S11). The resistance change of the GMR sensor was measured. The amount of IL-6 in the serum was then determined on the basis of the dose–response curve (Figure 3B).

Conclusions

In summary, we have developed an ultrasensitive, highly specific and reproducible, and rapid sensing platform with a wide detecting range. This platform consists of the integration

of a near 0 $^{\circ}$ GMR sensor with a uniform high-magnetic-moment FeCo nanoparticle-based device and a competition-based detecting principle. We demonstrated the feasibility of this system to directly quantify IL-6 in unprocessed human serum samples in 5 min. Although 4 μL of serum was used for this analysis, only 4 nL of the serum is indeed responsible for the signal, because we have not achieved sensor area-specific modification, in that the capture-antibody-modified area includes the sensor and its surrounding region. The surrounding region is ~ 1000 times the area of the sensor (see Supporting Information, p S10). Hence, upon achieving sensor-specific modification, our sensor platform would require only 4 nL of serum for detection, or it could quantify IL-6 from serum at a much lower IL-6 concentration, which is currently under investigation. The detecting specificity of this system was rigorously established by demonstrating that IL-6-depleted sera introduced no signal at all. Rapid detection (5 min) and reproducibility were also achieved for this system. Such a platform paves the practical way for the identification and validation of biomarkers involved in the etiology of various diseases. It may eventually lead to a low-cost and hand-held medical device for early detection of chronic diseases.

Acknowledgment. This work was partially supported by the Center for Nanostructured Application at University of Minnesota, National Science Foundation NSF BME 0730825 program, and Minnesota Mayo nanotechnology partnership in cancer translational research. Parts of this work were carried out in the Minnesota Characterization Facility, which receives partial support from NSF through NNIN and MRSEC programs.

Supporting Information Available: Experimental methods, optimization results from silica wafer surface modification experiments, and additional figures. This material is available free of charge via the Internet at <http://pubs.acs.org>.

JA910406A